Phys. Lett. B 877 (2026) 140477

Contents lists available at ScienceDirect

Physics Letters B

journal homepage: www.elsevier.com/locate/physletb

Letter

CP prediction from residual $\mathbb{Z}_2^s$ and $\overline{\mathbb{Z}}_2^s$ symmetries with the latest data

Shao-Feng Ge [a,b], Chui-Fan Kong [c], João Paulo Pinheiro [a,b]

[a] School of Physics & Astronomy, State Key Laboratory of Dark Matter Physics, Tsung-Dao Lee Institute, Shanghai Jiao Tong University, China
[b] Key Laboratory for Particle Astrophysics & Cosmology (MOE) & Shanghai Key Laboratory for Particle Physics & Cosmology, Shanghai Jiao Tong University, Shanghai, 200240, China
[c] Center for Theoretical Physics of the Universe (CTPU), Particle Theory and Cosmology Group (PTC), Institute for Basic Science, Daejeon, 34126, Republic of Korea

ARTICLE INFO

Editor: Prof Ryuichiro Kitano

Keywords:
Neutrino CP
Residual symmetry
Neutrino oscillation

ABSTRACT

The JUNO first data and the recent neutrino global fit results are implemented in the sum rule from the residual $\mathbb{Z}_2^s$ and $\overline{\mathbb{Z}}_2^s$ symmetries to make prediction of the leptonic Dirac CP phase δ_D. Without involving model parameters, the probability distribution of δ_D can be readily obtained from the experimental measurements of the three mixing angles. We then confront the theoretical predictions with the global fit results for the CP phase as well as the T2K and NOvA joint analysis for their CP measurements to give the data preference of the two residual symmetries with Bayes factor for both normal and inverted orderings. We further extend our analysis to a two-dimensional probability distribution to fully explore the correlation between the CP phase δ_D and the atmospheric angle $\theta_a \equiv \theta_{23}$.

1. Introduction

Neutrino oscillation is the first new physics beyond the Standard Model of particle physics with various solid experimental data [1]. It provides not just a key to understanding the possible new physics world beyond our current knowledge [2–5], but also a first observation of quantum interference phenomena at macroscopic lengths spanning from $\mathcal{O}(1)$ km at reactor experiments such as Daya Bay to $\mathcal{O}(10^5)$ km for solar neutrino transition.[1] With the Daya Bay [6], RENO [7], and Double Chooz [8] experiments establishing a nonzero $\theta_r(\equiv \theta_{13})$ mixing angle, neutrino physics has entered a precision era [9]. Especially, this allows possible measurement of the leptonic Dirac CP phase δ_D [10,11] that may hold the key to understanding why our Universe is made of matter but almost no anti-matter [12,13].

The mixing parameters will be measured with high precision at the new-generation neutrino experiments. Especially, the JUNO experiment can provide sub-percentage precision for $\theta_s(\equiv \theta_{12})$ and Δm_s^2 $(\equiv \Delta m_{21}^2)$ [14,15] with full data collection. This would allow further test of those flavor symmetries and models that can predict the neutrino mixing pattern.

A flavor symmetry is typically imposed on the fundamental Lagrangian of an ultra-violet (UV) complete theory as starting point [16–22]. Being an UV complete model, it should satisfy the electroweak gauge symmetries $SU(2)_L \times U(1)_Y$ with the left-handed neutrino $\nu_{\ell L}$ and its charged lepton counterpart ℓ_L in the same $SU(2)_L$ doublet $(\nu_{\ell L}, \ell_L)^T$. The flavor symmetry should be imposed on such doublet to respect the gauge symmetries. Then, the flavor symmetry has to be broken in order to allow the left-handed neutrinos and charged leptons to develop different mixing matrices U_ν and U_ℓ, respectively, such that the physical PMNS mixing matrix $U_{\rm PMNS} \equiv U_\ell^\dagger U_\nu$ can be nontrivial [23]. Such flavor symmetry breaking should happen at the same time as the electroweak symmetry breaking. So if there is any flavor symmetry that really dictates the neutrino mixing pattern, it has to be the residual symmetry [24] that survives the symmetry breaking processes.

After symmetry breaking, a residual symmetry should apply to the neutrino mass term whose diagonalization gives the mixing pattern. It turns out a direct connection can be established not just between the symmetry transformation G_ν and the neutrino mass matrix M_ν but actually between G_ν and the mixing matrix U_ν [24–27]. Then a correlation among the mixing parameters (including three mixing angles and one leptonic Dirac CP phase) can be established without involving any model parameters or the neutrino mass eigenvalues [28–30]. Study on such correlation was later further developed under the name of *Sum Rule*.

In this letter, we first summarize the major features and unique predictions of the residual $\mathbb{Z}_2^s$ or $\overline{\mathbb{Z}}_2^s$ symmetries for Majorana neutrinos. Since the Dirac CP phase has not been fully established, we emphasize its predicted values in terms of the already measured three mixing angles [29–31]. Especially, the JUNO experiment provides very precise measurement of the solar angle θ_s [32]. We show the current prediction

E-mail addresses: gesf@sjtu.edu.cn (S.-F. Ge), kongcf@ibs.re.kr (C.-F. Kong), joaopaulo.pinheiro@fqa.ub.edu (J.P. Pinheiro).

[1] Note that the 2025 Nobel Prize in Physics awards quantum phenomena at the centimeter scale.

https://doi.org/10.1016/j.physletb.2026.140477
Received 12 February 2026; Received in revised form 13 March 2026; Accepted 21 April 2026
Available online 24 April 2026
0370-2693/© 2026 The Author(s). Published by Elsevier B.V. Funded by SCOAP³. This is an open access article under the CC BY license (http://creativecommons.org/licenses/by/4.0/).

of δ_D has been significantly improved and make an explicit comparison with the latest measurement from the accelerator oscillation experiments [33].

2. Residual symmetries and CP correlation with mixing angles

As mentioned above, a residual symmetry is the one that survives the electroweak symmetry breaking to allow different mixing matrices for neutrinos and charged leptons. Since neutrinos become massive after symmetry breaking, the transformation matrix G_ν of a residual symmetry directly applies to the mass matrix M_ν,

$$G_\nu^T M_\nu G_\nu = M_\nu. \tag{1}$$

For simplicity, we have chosen the mass basis of charged leptons such that the PMNS matrix comes from the neutrino side alone. Note that the above symmetry transformation invariance of the mass matrix with a transposed G_ν^T applies for Majorana neutrinos.

The direct connection between a symmetry transformation matrix and the mass matrix is the essential feature of residual symmetries. If a symmetry is really the one that dictates the mixing pattern, it has to survive through the mass generation process and directly restricts the resulting mass matrix without interference from other factors such as Yukawa couplings and the vacuum expectation values.

The mass matrix M_ν of Majorana neutrinos in the flavor basis can be diagonalized as $U_\nu^T M_\nu U_\nu = D_\nu$ where $D_\nu \equiv \text{diag}\{m_1, m_2, m_3\}$ is the diagonal mass matrix in the mass basis, or equivalently, $M_\nu = U_\nu^* D_\nu U_\nu^\dagger$. Then one may replace the M_ν in Eq. (1) to obtain $G_\nu^T U_\nu^* D_\nu U_\nu^\dagger G_\nu = U_\nu^* D_\nu U_\nu^\dagger$. Although the neutrino mass eigenvalues m_i are involved, it is possible to obtain a mass indepenent solution,

$$U_\nu^\dagger G_\nu U_\nu = d_\nu, \quad \text{or} \quad G_\nu = U_\nu d_\nu U_\nu^\dagger. \tag{2}$$

Under the transformation of d_ν, the diagonal mass matrix D_ν should also be invariant, $d_\nu^T D_\nu d_\nu = D_\nu$ which requires the d_ν to be diagonal with only 8 possibilities, $d_\nu \equiv \text{diag}\{\pm1, \pm1, \pm1\}$. The diagonal transformation d_ν is actually the diagonal representation of the same residual $\mathbb{Z}_2$ symmetries in the mass basis.

It is interesting to observe that Eq. (2) is actually a direct connection between the residual transformation matrix G_ν and the neutrino mixing matrix U_ν. As indicated by the first equation therein, the mixing matrix U_ν can be obtained by diagonalizing G_ν. There is actually no need to first obtain the mass matrix M_ν and then diagonalize it to determine the mixing matrix U_ν. Instead of such two step procedure, the mixing pattern can be directly obtained from the residual symmetry transformation. The mixing pattern is really dictated by the residual symmetry without involving any other factors. If we take the relation in the other way around, the residual symmetry transformation matrix G_ν can be reconstructed in terms of the mixing matrix U_ν as explicitly shown by the second equation in Eq. (2). This is a very neat and direct connection between symmetry and observables.

Of the 8 possibilities of d_ν only two are independent, $d_\nu^{(1)} \equiv \text{diag}\{-1, 1, 1\}$ and $d_\nu^{(2)} \equiv \text{diag}\{1, -1, 1\}$. Correspondingly, the two residual transformation matrices are,

$$G_1(k) = \frac{1}{2+k^2}\begin{pmatrix} 2-k^2 & 2k & 2k \\ & k^2 & -2 \\ & & k^2 \end{pmatrix}, \tag{3a}$$

$$G_2(k) = \frac{1}{2+k^2}\begin{pmatrix} 2-k^2 & 2k & 2k \\ & -2 & k^2 \\ & & -2 \end{pmatrix}, \tag{3b}$$

where k is a free parameter. Both G_1 and G_2 are generators of a $\mathbb{Z}_2^s$ or $\overline{\mathbb{Z}}_2^s$ symmetry, respectively. Note that only one of these two $\mathbb{Z}_2$ symmetries can exist as residual symmetry, especially after the $\mu - \tau$ symmetry [34,35] that corresponds to $d_\nu^{(3)} \equiv \text{diag}\{1, 1, -1\}$ and $G_3 = G_1 G_2$ is broken.

Although it seems like both $G_1(k)$ and $G_2(k)$ contain a model parameter k, they can predict unique connection between the Dirac CP phase δ_D and three mixing angles, which are the atmospheric angle $\theta_a \equiv \theta_{23}$, the solar angle θ_s, and the reactor angle θ_r [29–31]:

$$\cos\delta_D = \frac{(s_s^2 - c_s^2 s_r^2)(s_a^2 - c_a^2)}{4 c_a s_a c_s s_s s_r}, \tag{4a}$$

$$\cos\delta_D = \frac{(s_s^2 s_r^2 - c_s^2)(s_a^2 - c_a^2)}{4 c_a s_a c_s s_s s_r}, \tag{4b}$$

for $\mathbb{Z}_2^s$ and $\overline{\mathbb{Z}}_2^s$, respectively. Here $s_{r,s,a} \equiv \sin\theta_{r,s,a}$ and $c_{r,s,a} \equiv \cos\theta_{r,s,a}$ denote the sine and cosine functions of the mixing angles. Since the $\mu - \tau$ symmetry dictates a vanishing reactor angle ($\theta_r = 0$) and maximal atmospheric angle ($\theta_a = \pi/4$), breaking it allows non-zero θ_a and $c_a^2 - s_a^2$. The ratio between these two deviations is correlated with the leptonic Dirac CP phase δ_D.

Although the transformation matrices $G_1(k)$ and $G_2(k)$ are functions of a model parameter k, the correlation above only involves physical observables in neutrino experiments. The property that a residual symmetry can establish connection among physical observables has a close analogy in the electroweak symmetry breaking. Although the SM $SU(2)_L \times U(1)_Y$ gauge symmetries are broken, the custodial symmetry predicts a correlation among the gauge boson masses (M_Z and M_W) and the weak mixing angle which are all physical observables. It is readily possible to use physical observations to justify such correlations. The residual symmetry for the neutrino mixing pattern has the same spirit as the custodial symmetry for the gauge mixing [36]. It is interesting to see that both cases have the concept of mixing pattern which is another similarity.

3. CP prediction with JUNO first data

The current global-fit result [37] has reached percentage level for the mixing angle measurement and provided mild constraint on the Dirac CP phase. In addition, the JUNO reactor neutrino experiment just released their first data with better measurement of solar angle, $s_s^2 = 0.3092 \pm 0.0087$ [32]. With this in mind, we would like to see how the updated measurements affect the CP phase prediction of the residual symmetry sum rules. Especially, how the theoretical predictions of the Dirac CP phase distribution compare with its current measurement result.

The probability distribution function of $\cos\delta_D$ can be expressed by integrating over the mixing angle distribution probabilities [30,31],

$$\frac{dP(\cos\delta_D)}{d\cos\delta_D} = \int \delta_D^p\, \mathbb{P}(s_r^2)\mathbb{P}(s_s^2)\mathbb{P}(s_a^2)\, ds_r^2\, ds_s^2\, ds_a^2, \tag{5}$$

where $\delta_D^p \equiv \delta(\cos\delta_D - \bar{c}_D)$ is a δ-function with $\bar{c}_D$ denoting the RHS of Eq. (4) to enforce the residual symmetry sum rule. The probability distribution function inside the integration $\mathbb{P}(s_r^2, s_s^2, s_a^2) \equiv \mathbb{P}(s_r^2)\mathbb{P}(s_s^2)\mathbb{P}(s_a^2)$ represents the prior probability distributions of (s_r^2, s_s^2, s_a^2) extracted from data or global fits. Then, the probability distribution of the Dirac CP phase δ_D can be obtained with a simple transformation and Jacobian,

$$\frac{dP(\delta_D)}{d\delta_D} = |\sin\delta_D| \frac{dP(\cos\delta_D)}{d\cos\delta_D}. \tag{6}$$

The prediction of the leptonic Dirac CP phase δ_D would sensitively depend on the input prior of mixing angles. In the presence of measurement uncertainties of mixing angles, the Dirac CP phase that predicted from the mixing angles is not a fixed value but follows a distribution. To calculate the predicted distribution of the Dirac CP phase from the mixing angles, we extract the NuFIT [37] one-dimensional distributions of the mixing angles.

As indicated by Eq. (4), the two deviations (θ_r and $c_a^2 - s_a^2$) from the tribimaximal mixing [38–40] are proportional to each other. With $|\cos\delta_D| \leq 1$ being limited from above, the reactor angle θ_r needs to be nonzero which has been firmly established by Daya Bay [41], RENO [42], and Double-Chooz [43] with high precision. Otherwise, neither deviations can happen. A nonzero reactor angle θ_r is really the key for going beyond the tribimaximal mixing. With the precision measurements

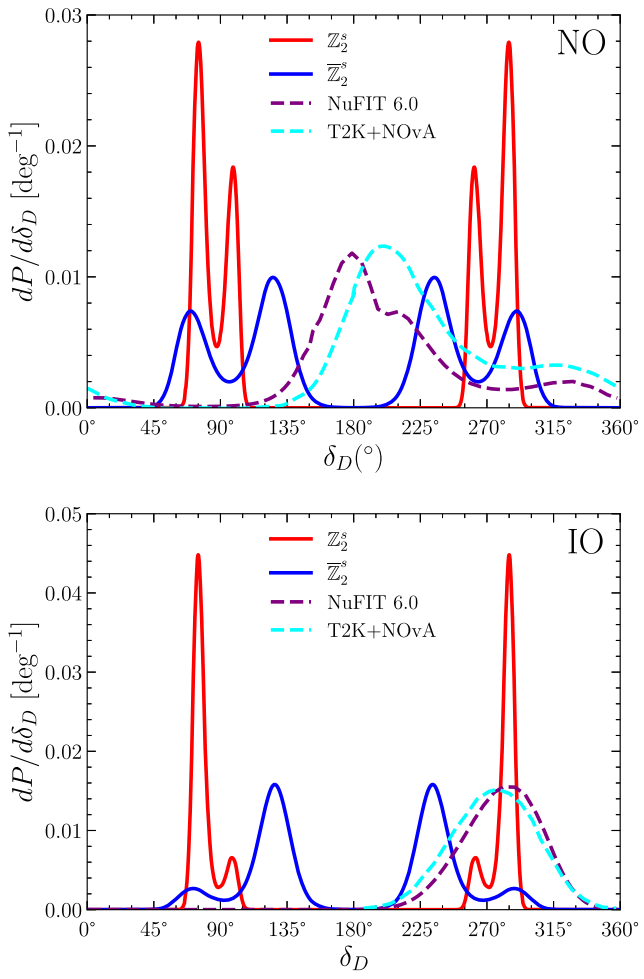

Fig. 1. The predicted probability distributions of the leptonic Dirac CP phase according to the residual $\mathbb{Z}_2^s$ (red) or $\overline{\mathbb{Z}}_2^s$ (blue) symmetries with inputs from the current NuFIT 6.0 global fit plus the JUNO first data release. In addition, the CP phase probability distributions from the NuFIT 6.0 global fit (purple dashed) and the T2K plus NOvA joint analysis (cyan dashed) are also shown for comparison. Both normal (NO) and inverted (IO) orderings have been shown in the upper and lower panels, respectively.

in the last 10 years, the uncertainty in $\sin^2\theta_r$ has decreased from roughly 10% to around 2.5%.

For these three mixing angles, we take their normalized distribution according to the corresponding χ^2 function, $\mathbb{P}(s^2_{a,r,s}) \propto \exp(-\chi^2/2)$. Note that the χ^2 functions of $s^2_{r,s}$ are almost symmetric and follow a parabola. Then, the probability distributions of $s^2_{r,s}$ can be described by a normalized Gaussian distribution function, $\mathbb{P}(s^2_{r,s}) \equiv \exp[-(s^2_{r,s;\mathrm{BF}} - s^2_{r,s})^2)/2\sigma^2_{s^2_{r,s}}]/\sqrt{2\pi}\sigma_{s^2_{r,s}}$. However, for the atmospheric angle, its distribution is asymmetric and has two local χ^2 minima [37]. In this case, we calculate the s^2_a distribution probabilities using its exact χ^2 function.

Fig. 1 shows the predicted probability distribution function with the latest NuFit [37] plus the JUNO first data [32] (solid) for both $\mathbb{Z}_2^s$ (red) and $\overline{\mathbb{Z}}_2^s$ (blue). In comparison with the previous results [31], the predicted CP distribution shrinks quite significantly. This is a manifestation of the fact that the experimental uncertainties on the mixing angles have improved quite a lot.

It is instructive to examine how the experimental uncertainty in θ_s propagates into the prediction of $\cos\delta_D$. Neglecting the tiny s^2_s in the numerator, the sum rules in Eq. (4) are roughly modulated by the solar mixing angle as $\tan\theta_s$ (for $\mathbb{Z}_2^s$) and $\cot\theta_s$ (for $\overline{\mathbb{Z}}_2^s$). For a small perturbation $\delta\theta_s$ in the solar angle, both tangent and cotangent propagate errors with the same amplification factor $\sim 2\delta\theta_s/\sin(2\theta_s)$, leading to a relative uncertainty in $\cos\delta_D$ that is amplified by $\sim 2/\sin(2\theta_s)$ compared to the relative uncertainty in θ_s itself. For the JUNO first measurement, this amplification factor is ~ 2.16. The improved precision from JUNO, reducing the relative uncertainty in θ_s from $\sim 4\%$ to $\sim 2.16\%$, would improve the precision of the predicted $\cos\delta_D$ by a factor of two from 8.6% to 4.7%.

Comparing the solid curves that represent the updated prediction of the δ_D distribution with the previous results in 2013 [31], the updated predictions have two local peaks. Such a feature arises from the two local minima in the χ^2 distribution function of s^2_a. To be more exact, the atmospheric angle θ_a has two local best-fit values in the lower ($\theta_a < \pi/4$) or higher ($\theta_a > \pi/4$) octants. According to Eq. (4), switching octant for θ_a would lead to a minus sign in the predicted $\cos\theta_D$ and hence δ_D becomes $\pi - \delta_D$. This explains why the two peaks mirror around the maximal CP point $\delta_D = \pm\pi/2$. However, such mirror symmetry is not exact since the two octant solutions of θ_a have different probabilities or weights [9,37]. For NO, the two peaks have comparable heights while the IO case has a much larger disparity. But the previous results in 2013 are dominated by a single peak for the NO case, although the IO case has more sizable second peak. It seems that from the 2013 results to the updated, the situation on the atmospheric angle octant switches between NO and IO.

Moreover, since the sum rule in Eq. (4) is determined by $\cos\delta_D$, the determination of the CP phase becomes symmetric between the $[0,\pi]$ and $[\pi,2\pi]$ regions. As illustrated in Fig. 1, this dependence leads to an explicit degeneracy between δ_D and $2\pi - \delta_D$ (or equivalently $-\delta_D$). This cosine dependence arises because the residual $\mathbb{Z}_2$ symmetries in vacuum impose sum rules that fix δ_D via relations like $|U^{\mathrm{vac}}_{\mu i}| = |U^{\mathrm{vac}}_{\tau i}|$, making the solutions with opposite signs of δ_D [44] indistinguishable. However, the $\nu_\mu \to \nu_e$ transition probability at long-baseline experiments is sensitivity to $\sin\delta_D$ and can break this degeneracy. In realistic scenarios where neutrinos propagate through matter, this degeneracy is further lifted as the matter potential breaks the underlying vacuum symmetry. Long-baseline experiments such as DUNE [45] and T2HK [46] will exploit this matter-induced breaking of the vacuum symmetry to resolve the degeneracy in δ_D, allowing symmetry models to be tested against a unique determination of the CP-violating phase [47,48].

In addition, the major peak predicted by $\mathbb{Z}_2^s$ is below the maximal CP point, $\delta_D < \pi/2$ (or $\delta_D > -\pi/2$) for the updated results. This corresponds to a positive $\cos\delta_D$ with $s^2_a > c^2_a$ ($\theta_a > \pi/4$) accordingly to Eq. (4) which is consistent with the preferred higher octant best fit of θ_a. The major peak moves above the maximal CP point for the $\overline{\mathbb{Z}}_2^s$ case since the first parenthesis in Eq. (4) switches sign between the two residual symmetries. Moreover, the sum rule from the $\overline{\mathbb{Z}}_2^s$ residual symmetry gives a broader δ_D distribution than the $\mathbb{Z}_2^s$ case.

It is interesting to see that for all cases, a vanishing CP effect (δ_D is either 0 or π) is not highly disfavored by the two residual symmetries. Although the maximal CP phase point ($\delta_D = \pm\pi/2$) does not have the highest probability since $\theta_a = \pi/4$ is not favored by data, the two peaks are quite close to it. This is a very important and distinct feature that we can already conclude with the current data. The residual $\mathbb{Z}_2^s$ and $\overline{\mathbb{Z}}_2^s$ symmetries prefer non-vanishing CP with probably a sizable value. Let us take perturbative expansion around the tribimaximal mixing pattern, $\theta_r \equiv \delta_r$ is small and $\theta_a \equiv \pi/4 + \delta_a$ with both δ_r and δ_a denoting the deviations. Up to the linear order, Eq. (4) becomes [30],

$$\mathbb{Z}_2^s : \cos\delta_D \approx \frac{s_s}{c_s}\frac{\delta_a}{\delta_r}, \quad \overline{\mathbb{Z}}_2^s : \cos\delta_D \approx -\frac{c_s}{s_s}\frac{\delta_a}{\delta_r}, \tag{7}$$

The current best-fit gives $\delta_r = 8.52^\circ$ (8.57°) and $\delta_a = 3.50^\circ$ (3.56°) for NO (IO) [37]. For both mass orderings, the ratio between the two deviations $\delta_a/\delta_r \approx 0.4$ cannot be compensated with the prefactor $\tan\theta_s/2 \approx 0.33$ for $\mathbb{Z}_2^s$ or $\cot\theta_s/2 \approx 0.75$ for $\overline{\mathbb{Z}}_2^s$ to make $\cos\delta_D$ close enough to 1. A non-

Table 1
Bayesian evidence $P(D|M)$ and Bayes Factors BF $\equiv P(D|\mathbb{Z}_2^s)/P(D|\overline{\mathbb{Z}}_2^s)$ with inputs from the NuFIT 6.0 (T2K-NOvA joint analysis) and the JUNO first data. For the analysis with both orderings, we are assuming equal probability for normal and inverted ordering.

	Symmetry	BF (1D)	BF (2D)
NO	$\frac{\mathbb{Z}_2^s}{\overline{\mathbb{Z}}_2^s}$	0.42 (0.59)	0.30
IO	$\frac{\mathbb{Z}_2^s}{\overline{\mathbb{Z}}_2^s}$	2.11 (2.02)	2.40
NO & IO	$\frac{\mathbb{Z}_2^s}{\overline{\mathbb{Z}}_2^s}$	1.18 (1.13)	1.35

vanishing leptonic Dirac CP phase is guaranteed by the residual $\mathbb{Z}_2^s$ and $\overline{\mathbb{Z}}_2^s$ symmetries.

Besides the theoretical prediction of δ_D distribution from the sum rule, the experimental side also provides a δ_D distribution. The first measurement of the Dirac CP phase was published by T2K [49] and NOvA [50] in 2019. Very recently, the T2K and NOvA collaborations have also published their combined analysis [33], shown as cyan dashed curves in Fig. 1, based on their recent measurements [51,52]. Correspondingly, the global fit group updated the NuFIT 6.0 result [37] in 2024 which is shown as purple dashed curves. The CP distributions are consistent between the global-fit result and T2K-NOvA joint analysis result in the case of IO, while for NO the CP distribution from the joint result is slightly shifted to the right-handed side. As shown in the figure, the best-fit values differ between the NO and IO cases. While IO prefers a maximal CP phase $\delta_D \approx 280°$, NO prefers an almost vanishing one $\delta_D \approx 180°$. Moreover, the NO has a broader distribution than the IO case due to the existing tension between T2K and NOvA results.

To quantify the preference of the theoretical predictions of a model M by a CP measurement data set D, we take the Bayesian method [53] and define the following marginal likelihood,

$$P(D|M) \equiv \int \mathbb{P}(D|f_\delta^M)\mathbb{P}(s_r^2)\mathbb{P}(s_s^2)\mathbb{P}(s_a^2)\,\mathrm{d}s_r^2\,\mathrm{d}s_s^2\,\mathrm{d}s_a^2, \tag{8}$$

where $f_\delta^M \equiv \delta_D(s_r^2, s_s^2, s_a^2)|_M$ is the theoretical prediction from the residual symmetry as a function of the three mixing angles and $\mathbb{P}(D|f_\delta^M)$ is the probability distribution imposed by the data D. Comparing with Eq. (5), the δ_D^p function for imposing a fixed-value for the Dirac CP phase which is a very special probability distribution is replaced by a more realistic $\mathbb{P}(D|f_\delta^M)$ with spread. If all the probability distribution functions $\mathbb{P}$ extracted from data follow the Gaussian distribution, after integration $P(D|M)$ is actually a manifestation of the $\chi^2_{\rm min}$ that quantifies the extent of fitting a data set D with model M. A larger value of $P(D|M)$, which corresponds to a smaller $\chi^2_{\rm min}$, means better fitting. To quantitatively compare the preference of data between the two residual symmetries, we adopt the Bayes factor, BF $\equiv P(D|\mathbb{Z}_2^s)/P(D|\overline{\mathbb{Z}}_2^s)$. To make it more explicit, a BF > 1 prefers $\mathbb{Z}_2^s$ and BF < 1 means that $\overline{\mathbb{Z}}_2^s$ has a better change. The two models have equal preference when BF $= 1$.

Our result of the Bayesian factor is summarized in the BF (1D) column of Table 1 with inputs from the NuFIT 6.0 (T2K-NOvA joint analysis) [37] and the JUNO first data [32]. For NO, the global-fit result prefers $\overline{\mathbb{Z}}_2^s$ which is consistent with Fig. 1 where the purple dashed curve has a larger overlap with the blue solid curve for $\overline{\mathbb{Z}}_2^s$ than the red solid one for $\mathbb{Z}_2^s$. In the case of IO, the data prefers $\mathbb{Z}_2^s$ since the purple dashed curve overlaps more with red solid curve than its blue solid counterpart. It is also interesting to see that the peak position of the red solid curve is consistent with the purple dashed one, which means the theoretically predicted δ_D value from $\mathbb{Z}_2^s$ is very consistent with the measurement. Note that the preference on the theoretical models with input from the T2K-NOvA joint analysis is slightly reduced than the global-fit case.

Moreover, since the global-fit result has a light preference for NO, we also present the combined Bayes factor,

$$P(D|M) \equiv p_{\rm NO} \times P(D|M)_{\rm NO} + p_{\rm IO} \times P(D|M)_{\rm IO}, \tag{9}$$

to take into account the mass ordering weight factors $p_{\rm NO} = 0.574$ and $p_{\rm IO} = 0.426$.[2] The combined mass ordering analysis shows that the global-fit result has only a mild preference for $\mathbb{Z}_2^s$. The results in the table show opposite preferences between the NO and IO cases. We expect the mass ordering to be resolved with JUNO final result [15].

4. Correlation between Dirac CP phase δ_D and atmospheric angle θ_a

Besides the predicted δ_D distribution from the sum rule as given in Eq. (6), it is interesting to consider the correlation behavior between δ_D and mixing angles. As reported in the current NuFIT result [37], the Dirac CP phase δ_D and the atmospheric angle s_a^2 are correlated, which can be seen in their two-dimensional χ^2 distribution, shown as light (68% C.L.) and dark (95% C.L.) green contours in Fig. 2. The best-fit points are shown with a red star for both mass orderings. There exists a slightly negative correlation between δ_D and s_a^2 for NO and a positive one for IO. Such information can also be useful for testing the residual $\mathbb{Z}_2^s$ and $\overline{\mathbb{Z}}_2^s$ symmetries.

To obtain the correlation from the sum rules, we insert an additional $\delta(s_a^2 - s_{a,\rm fix}^2)$ to fix s_a^2 in Eq. (5). Then only uncertainties of s_r^2 and s_s^2 are taken into account. For each fixed s_a^2, one may obtain a 95% C.L. range for the sum rule prediction of δ_D. Varying the fixed s_a^2, a narrow band for the predicted δ_D as function of the atmospheric angle s_a^2 can be formed for $\mathbb{Z}_2^s$ (red) and $\overline{\mathbb{Z}}_2^s$ (blue), respectively. One may see that the correlation behavior is opposite between $\mathbb{Z}_2^s$ and $\overline{\mathbb{Z}}_2^s$ predictions which is independent on the mass ordering. The predicted δ_D deviates from π with an increasing s_a^2 for $\mathbb{Z}_2^s$ (red) and the opposite for $\overline{\mathbb{Z}}_2^s$ (blue). Such difference in the correlation behavior arises from the different factors in Eq. (4), which is $s_s^2 - c_s^2 s_r^2$ for $\mathbb{Z}_2^s$ and $s_s^2 s_r^2 - c_s^2$ for $\overline{\mathbb{Z}}_2^s$. It becomes more explicit with the sign difference between the two expanded forms in Eq. (7). Moreover, the best-fit values and the corresponding uncertainties of s_r^2 and s_s^2 are almost the same between NO and IO. As a result, the blue or red contours in Fig. 2 are quite similar between the NO and IO cases. The octant of θ_a remains unknown and constitutes the dominant source of uncertainty in the prediction of δ_D. The next-generation experiments, such as DUNE [45] and T2HK [46], aim to resolve this octant degeneracy and significantly improve the precision of the δ_D prediction.

When comparing the theoretical prediction with the global fit contours, it is interesting to see that the $\mathbb{Z}_s^2$ symmetry has a positive correlation between δ_D and s_a^2 for the $\delta_D > \pi$ branch which is the consistent as the global-fit result for IO. In addition, the $\overline{\mathbb{Z}}_2^s$ symmetry for $\delta_D > \pi$ has a positive correlation that is consistent with the global-fit result for NO.

As mentioned above, we take the Bayesian factor to quantify the global-fit result preference on the theoretical models. Here we take the two-dimensional probability distribution of the atmospheric angle s_a^2 and the leptonic Dirac CP phase δ_D as data set D to evaluate $P(D|M)$ in the similar way as defined in Eq. (8). In such a way, the correlation between s_a^2 and δ_D can be fully taken into account. The results are summarized in the BF (2D) column of Table 1. Taking this two-dimensional analysis into account, the preference of $\mathbb{Z}_2^s$ with NO decreases while the preference of $\overline{\mathbb{Z}}_2^s$ increase in the IO case. This is consistent with the contour plots in Fig. 2 where $\overline{\mathbb{Z}}_2^s$ ($\mathbb{Z}_2^s$) has negative (positive) correlation for NO (IO) which are consistent with the NuFIT 6.0 contours. If both

[2] For the NuFIT 6.0 result, there is a $\Delta\chi^2 = 0.6$ preference for NO. This preference can be translated into priors $p_{\rm NO}$ and $p_{\rm IO}$. $\Delta\chi^2 = \chi^2_{\rm NO} - \chi^2_{\rm IO} = 0.6 \to \mathcal{L}_{\rm NO}/\mathcal{L}_{\rm IO} = \exp(-0.3) = 0.741$. Fixing $\mathcal{L}_{\rm NO} = 1$, the relative thickness $p_{\rm NO} = 1/(1 + 0.741) = 0.574$ and $p_{\rm IO} = 0.741/(1 + 0.741) = 0.426$.

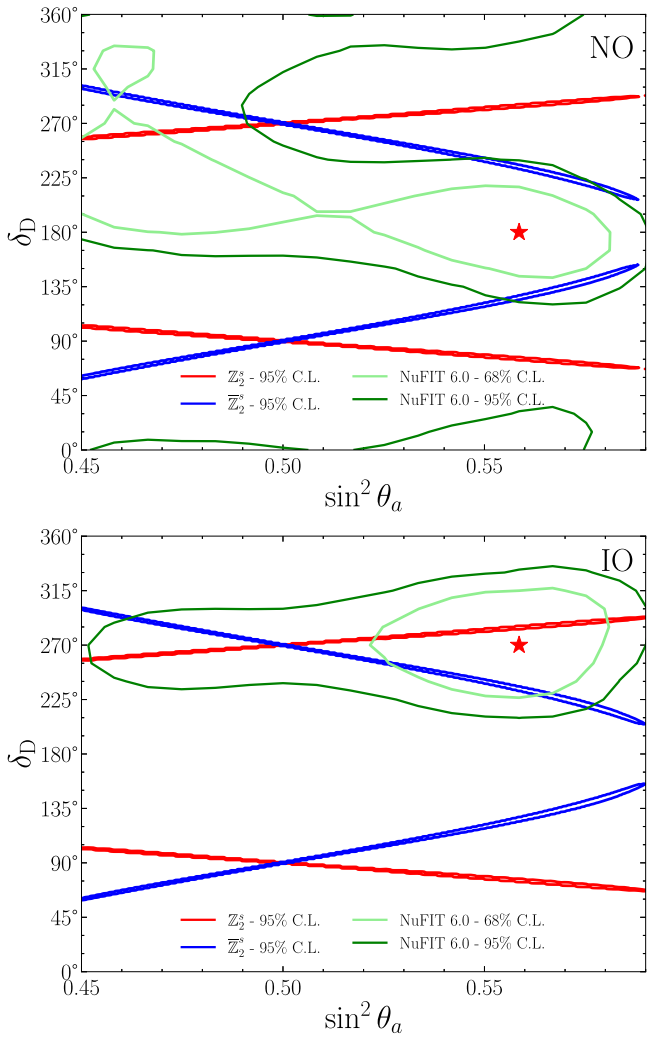

Fig. 2. Comparison between the theoretical prediction of the residual $\mathbb{Z}_2^s$ (red) or $\overline{\mathbb{Z}}_2^s$ (blue) symmetries and the latest NuFIT 6.0 results (green) for the two-dimensional correlated probability distributions between the atmospheric angle θ_a and the leptonic Dirac CP phase δ_D. The upper panel is for NO while the lower one is for IO.

mass orderings are taken into a combined analysis, the preference for $\mathbb{Z}_2^s$ decreases.

5. Conclusion

The residual symmetry is by definition the one that can survive symmetry breaking and apply to the neutrino mass matrix to directly dictate the mixing pattern. A unique prediction of the residual $\mathbb{Z}_2^s$ and $\overline{\mathbb{Z}}_2^s$ symmetries is a correlation among the three mixing angles and the leptonic Dirac CP phase δ_D without involving model parameters. Later named as sum rule, such correlation involving only physical observables takes the same spirit as the correlation between weak gauge boson masses and the weak mixing angle that is predicted by the custodial symmetry that also survives the weak symmetry breaking.

With the updated global fit and the JUNO first data release, the CP prediction by the custodial symmetries has much smaller uncertainty now. In particular, the vanishing CP case ($\delta_D = 0$ or π) is theoretically excluded now and the predicted CP distribution peaks around the maximal CP value ($\delta_D = \pm\frac{\pi}{2}$). Since the experimental measurements have dependence on the neutrino mass ordering, the residual $\mathbb{Z}_2^s$ and $\overline{\mathbb{Z}}_2^s$ symmetries are preferred by IO and NO, respectively. The two-dimensional probability distribution of δ_D and the atmospheric angle θ_a with correlation can help distinguishing these two residual symmetries. Moreover, breaking the θ_a octant degeneracy remains crucial for giving more definite prediction of δ_D by eliminating the current double-peaked structure in the probability distributions to yield a single sharpe peak for each residual symmetry.

Data availability

Data will be made available on request.

Declaration of competing interest

The authors declare that they have no known competing financial interests or personal relationships that could have appeared to influence the work reported in this paper.

Acknowledgements

The authors would like to thank Yue Meng for useful discussions. The authors are supported by the National Natural Science Foundation of China (12425506, 12375101, 12090060 and 12090064) and the SJTU First Class start-up fund (WF220442604). CFK is supported by IBS under the project code IBS-R018-D1. SFG is also an affiliate member of Kavli IPMU, University of Tokyo.

References

[1] M.C. Gonzalez-Garcia, M. Yokoyama, "Neutrino masses, mixing, and oscillations", (Chapter 14) of S. Navas et al. [Particle Data Group], "Review of particle Physics", Phys. Rev. D 110 (2024), 030001
[2] M.S. Athar, S.W. Barwick, T. Brunner, J. Cao, M. Danilov, K. Inoue, T. Kajita, M. Kowalski, M. Lindner, K.R. Long, Status and perspectives of neutrino physics, Prog. Part. Nucl. Phys. 124 (2022) 0103947. arXiv:2111.07586 [hep-ph]
[3] C.A. Argüelles, G. Barenboim, M. Bustamante, P. Coloma, P.B. Denton, I. Esteban, Y. Farzan, E.F.M. ńez, D.V. Forero, A.M. Gago, Snowmass white paper: beyond the standard model effects on neutrino flavor: submitted to the proceedings of the US community study on the future of particle physics (Snowmass 2021), Eur. Phys. J. C 83 (1) (2021) 15. arXiv:2203.10811 [hep-ph]
[4] A.D. Gouvêa, I. Mocioiu, S. Pastore, L.E. Strigari, L. Alvarez-Ruso, A.M. Ankowski, A.B. Balantekin, V. Brdar, M. Cadeddu, S. Carey, Theory of Neutrino Physics - Snowmass TF11 (aka NF08) Topical Group Report. arXiv:2209.07983 [hep-ph]
[5] P. Huber, K. Scholberg, E. Worcester, J. Asaadi, A.B. Balantekin, N. Bowden, P. Coloma, P.B. Denton, A.D. Gouvêa, L. Fields, Snowmass Neutrino Frontier Report. arXiv:2211.08641 [hep-ex]
[6] F.P. An, [Daya Bay] Observation of electron-antineutrino disappearance at Daya Bay, Phys. Rev. Lett. 108 (2012) 171803. arXiv:1203.1669 [hep-ex]
[7] J.K. Ahn, [RENO] Observation of reactor electron antineutrino disappearance in the RENO experiment, Phys. Rev. Lett. 108 (2012) 191802. arXiv:1204.0626 [hep-ex]
[8] Y. Abe, Indication of reactor $\bar{\nu}_e$ disappearance in the double chooz experiment, [Double Chooz] Phys. Rev. Lett. 108 (2012) 131801. arXiv:1112.6353 [hep-ex]
[9] G.L. Fogli, E. Lisi, A. Marrone, D. Montanino, A. Palazzo, A.M. Rotunno, Global analysis of neutrino masses, mixings and phases: entering the era of leptonic CP violation searches, Phys. Rev. D 86 (2012). 013012. arXiv:1205.5254 [hep-ph]
[10] G.C. Branco, R.G. Felipe, F.R. Joaquim, Leptonic CP violation, Rev. Mod. Phys. 84 (2012) 515–565. arXiv:1111.5332 [hep-ph]
[11] P.A.N. Machado, H. Minakata, H. Nunokawa, R.Z. Funchal, What can we learn about the lepton CP phase in the next 10 years?, JHEP 05 (109) (2014). arXiv:1307.3248 [hep-ph]
[12] S. Davidson, E. Nardi, Y. Nir, Leptogenesis, Phys. Rept. 466 (2008) 105–177. arXiv:0802.2962 [hep-ph]
[13] P, D. Bari, An introduction to leptogenesis and neutrino properties, Contemp. Phys. 53 (4) (2012) 315–338. arXiv:1206.3168 [hep-ph]
[14] S.F. Ge, K. Hagiwara, N. Okamura, Y. Takaesu, Determination of mass hierarchy with medium baseline reactor neutrino experiments, JHEP (05) (2013) 131. arXiv:1210.8141 [hep-ph]
[15] F. An, [JUNO] Neutrino physics with JUNO, J. Phys. G 43 (3) (2016), 030401. arXiv:1507.05613 [physics.ins-det]
[16] G. Altarelli, F. Feruglio, L. Merlo, Tri-bimaximal neutrino mixing and discrete flavour symmetries, Fortsch. Phys. 61 (2013) 507–534. arXiv:1205.5133 [hep-ph]
[17] S.F. King, C. Luhn, Neutrino mass and mixing with discrete symmetry, Rept. Prog. Phys. 76 (2013), 056201. arXiv:1301.1340 [hep-ph]
[18] S.F. King, Unified models of neutrinos, flavour and CP violation, Prog. Part. Nucl. Phys. 94 (2017) 217–256. arXiv:1701.04413 [hep-ph]
[19] S.T. Petcov, Discrete flavour symmetries, neutrino mixing and leptonic CP violation, Eur. Phys. J. C 78 (9) (2018). arXiv:1711.10806 [hep-ph]
[20] Z.Z. Xing, Flavor structures of charged fermions and massive neutrinos, Phys. Rept. 854 (2020) 1–147. arXiv:1909.09610 [hep-ph]

[21] F. Feruglio, A. Romanino, Lepton flavor symmetries, Rev. Mod. Phys. 93 (1) (2021), 015007. arXiv:1912.06028 [hep-ph]
[22] G.J. Ding, S.F. King, Neutrino mass and mixing with modular symmetry, Rept. Prog. Phys. 87 (8) (2024), 084201. arXiv:2311.09282 [hep-ph]
[23] C.S. Lam, Neutrino 2-3 symmetry and inverted hierarchy, Phys. Rev. D 71 (2005), 093001. arXiv:hep-ph/0503159 [hep-ph]
[24] C.S. Lam. Symmetry of lepton mixing, Phys. Lett. B 656 (2007) 193–198. arXiv:0708.3665 [hep-ph]
[25] C.S. Lam, Mass independent textures and symmetry, Phys. Rev. D 74 (2006) 113004. arXiv:hep-ph/0611017 [hep-ph]
[26] C.S. Lam, Determining horizontal symmetry from neutrino mixing, Phys. Rev. Lett. 101 (2008) 121602. arXiv:0804.2622 [hep-ph]
[27] C.S. Lam, The unique horizontal symmetry of leptons, Phys. Rev. D 78 (2008), 073015. arXiv:0809.1185 [hep-ph]
[28] D.A. Dicus, S.F. Ge, W.W. Repko, Generalized hidden $\mathcal{Z}_2$ symmetry of neutrino mixing, Phys. Rev. D 83 (2011), 093007. arXiv:1012.2571 [hep-ph]
[29] S.F. Ge, D.A. Dicus, W.W. Repko, $\mathbb{Z}_2$ Symmetry prediction for the leptonic Dirac CP phase, Phys. Lett. B 702 (2011) 220–223. arXiv:1104.0602 [hep-ph]
[30] S.F. Ge, D.A. Dicus, W.W. Repko, Residual symmetries for neutrino mixing with a large θ_{13} and nearly maximal δ_D, Phys. Rev. Lett. 108 (2012), 041801. arXiv:1108.0964 [hep-ph]
[31] A.D. Hanlon, S.F. Ge, W.W. Repko, Phenomenological consequences of residual $\mathbb{Z}_2^s$ and $\overline{\mathbb{Z}}_2^s$ symmetries, Phys. Lett. B 729 (2014) 185–191. arXiv:1308.6522 [hep-ph]
[32] A. Abusleme, [JUNO] First Measurement of Reactor Neutrino Oscillations at JUNO. arXiv:2511.14593 [hep-ex]
[33] S. Abubakar, [T2K and NOvA] Joint neutrino oscillation analysis from the T2K and NOvA experiments, Nature 646 (8086) (2025) 818–824. arXiv:2510.19888 [hep-ex]
[34] Z.Z. Xing, Z.H. Zhao, A review of $\mu - \tau$ flavor symmetry in neutrino physics, Rept. Prog. Phys. 79 (7) (2016) 076201. arXiv:1512.04207 [hep-ph]
[35] Z.Z. Xing. The $\mu\tau$ reflection symmetry of Majorana neutrinos *, Rept. Prog. Phys. 86 (7) (2023) 076201. arXiv:2210.11922 [hep-ph]
[36] S.F. Ge, Unifying Residual $\mathbb{Z}_2^{23} \otimes \mathbb{Z}_2^{12}$ Symmetries and Quark-Lepton Complementarity. arXiv:1406.1985 [hep-ph]
[37] I. Esteban, M.C. Gonzalez-Garcia, M. Maltoni, I. Martinez-Soler, J.P. Pinheiro, T. Schwetz, NuFit-6.0: updated global analysis of three-flavor neutrino oscillations, JHEP 12 (2024) 216. arXiv:2410.05380 [hep-ph]
[38] P.F. Harrison, D.H. Perkins, W.G. Scott, Tri-bimaximal mixing and the neutrino oscillation data, Phys. Lett. B 530 (2002) 167. arXiv:hep-ph/0202074 [hep-ph]
[39] Z.Z. Xing, Nearly tri bimaximal neutrino mixing and CP violation, Phys. Lett. B 533 (2002) 85–93. arXiv:hep-ph/0204049 [hep-ph]
[40] X.G. He, A. Zee, Some simple mixing and mass matrices for neutrinos, Phys. Lett. B 560 (2003) 87–90. arXiv:hep-ph/0301092 [hep-ph]
[41] F.P. An et al. [Daya Bay], Precision measurement of reactor antineutrino oscillation at kilometer-scale baselines by Daya Bay, Phys. Rev. Lett. 130 (16) (2023) 161802. arXiv:2211.14988 [hep-ex]
[42] C. Shin, [RENO] Recent results from RENO, PoS ICHEP2020 (2021) 177.
[43] P. Soldin, [Double Chooz] Precision neutrino mixing angle measurement with the double chooz experiment and latest results, PoS TAUP2023 (2024) 228.
[44] M.J.S. Yang, A rephasing invariant formula for the Dirac CP phase and general perturbative expansion: prospects for DUNE and T2HK, Phys. Lett. B 868 (2025) 139784. arXiv:2507.04720 [hep-ph]
[45] R. Acciarri et al. [DUNE], Long-Baseline Neutrino Facility (LBNF) and Deep Underground Neutrino Experiment (DUNE): Conceptual Design Report, Volume 2: The Physics Program for DUNE at LBNF. arXiv:1512.06148 [physics.ins-det]
[46] K. Abe et al. [Hyper-Kamiokande], Hyper-Kamiokande Design Report. arXiv:1805.04163 [physics.ins-det]
[47] Y.H. Ahn, S.K. Kang, R. Ramos, M. Tanimoto, Confronting the prediction of leptonic Dirac CP-violating phase with experiments, Phys. Rev. D 106 (9) (2022) 095002. arXiv:2205.02796 [hep-ph]
[48] M. Tanimoto, T.T. Yanagida, Prediction of the CP phase δ_{CP} in the neutrino oscillation and an axion-less solution to the strong CP problem, PTEP 2025 (3) (2025) 033B01. arXiv:2410.01224 [hep-ph]
[49] K. Abe et al. [T2K], Constraint on the matterantimatter symmetry-violating phase in neutrino oscillations, Nature 580 (7803) (2020) 339–344. [erratum: Nature 583, no.7814, E16 (2020)]. arXiv:1910.03887 [hep-ex]
[50] M.A. Acero et al. [NOvA], First measurement of neutrino oscillation parameters using neutrinos and antineutrinos by NOvA, Phys. Rev. Lett. 123 (15) (2019) 151803. arXiv:1906.04907 [hep-ex]
[51] K. Abe et al. [T2K], Measurements of neutrino oscillation parameters from the T2K experiment using 3.6×10^{21} protons on target, Eur. Phys. J. C 83 (9) (2023) 782. arXiv:2303.03222 [hep-ex]
[52] M.A. Acero, [NOvA] Improved measurement of neutrino oscillation parameters by the NOvA experiment, Phys. Rev. D 106 (3) (2022) 032004. arXiv:2108.08219 [hep-ex]
[53] D.S. Sivia, J. Skilling, Data Analysis: A Bayesian Tutorial, ISBN 0-19-856831-2 Oxford University Press, 2006.